

See discussions, stats, and author profiles for this publication at: <https://www.researchgate.net/publication/14778587>

Use of Capillary Electrophoresis to Determine Kinetic and Equilibrium Constants for Binding of Arylsulfonamides to Bovine Carbonic Anhydrase

ARTICLE *in* JOURNAL OF MEDICINAL CHEMISTRY · FEBRUARY 1993

Impact Factor: 5.45 · DOI: 10.1021/jm00053a016 · Source: PubMed

CITATIONS

149

READS

16

4 AUTHORS, INCLUDING:



Erich Blossey

Rollins College

31 PUBLICATIONS 727 CITATIONS

SEE PROFILE

Use of Affinity Capillary Electrophoresis To Determine Kinetic and Equilibrium Constants for Binding of Arylsulfonamides to Bovine Carbonic Anhydrase¹

Luis Z. Avila, Yen-Ho Chu, Erich C. Blossey,² and George M. Whitesides*

Department of Chemistry, Harvard University, 12 Oxford Street, Cambridge, Massachusetts 02138

Received August 24, 1992

Affinity capillary electrophoresis (ACE) provides a new approach to studying protein-ligand interactions. The basis for ACE is the change in the electrophoretic mobility of the protein when it forms a complex with its ligand. This binding interaction can be quantified directly for charged ligands or indirectly for neutral ligands in competition with a previously characterized charged ligand. Determination of kinetic and equilibrium constants using ACE relies only on the changes in the migration time and shape (but not the area) of the peak due to protein. Simulation of the protein mobility under conditions of ACE suggests that the experimentally obtained electropherograms can be explained in terms of few variables: *on* and *off* rates (and thus, binding constant), concentration of the ligand(s), and relative mobilities of the protein and its complex(es).

Introduction

Affinity capillary electrophoresis (ACE)³⁻⁵ can be used to determine the binding constants, K_b , and kinetic constants, k_{on} and k_{off} , for the interaction of proteins with ligands. ACE is attractive because the procedures are rapid and only small quantities of protein and ligands are required. The potential of ACE to provide simultaneous evaluation of binding and kinetic constants of enzyme-inhibitor interactions is especially appealing when taken in the context of methodologies for generating and screening drug candidates. The effectiveness of a molecule as an enzyme inhibitor, and thus possibly as a drug, may depend not only on how tightly the inhibitor is bound by the enzyme but also on the rate of association of the enzyme and the inhibitor and the rate of dissociation of the enzyme-inhibitor complex.⁶

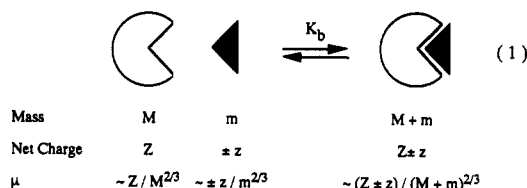
Here we describe several useful protocols for these analyses using as a model system carbonic anhydrase (CA, EC 4.2.1.1) as enzyme and arylsulfonamides as inhibitors. In principle these procedures can be used for analysis of binding in other systems of protein and ligands, provided that protein adsorption on the surface of the capillary is not significant and that a charged ligand is available or can be synthesized.

There are two types of procedures. Determination of thermodynamic binding constants involving measuring changes in mobility of the protein as a function of the concentration of a ligand (or ligands) in the electrophoresis buffer. We describe two variations in the procedure for studying protein-ligand interactions: in one, the protein interacts with a *single* charged ligand; in the second case, the protein interacts with a mixture of *two* ligands, one charged and one electrically neutral. The first procedure yields the binding constant of the charged ligand directly. The second allows the measurement of the binding constant of the neutral ligand, relative to the charged one, and thus provides a protocol for measuring binding constants of uncharged ligands. Both of these types of procedure involve only measurements of the positions of peaks (that is, migration times t_m). The intensity and the shape of the peak are not required.

This paper also describes a procedure for analyzing the displacement and shape of the protein peak, using a simple computer-based simulation, to obtain information concerning the kinetics of the interaction between the protein

and the ligand(s). In this procedure, matching of experimental and calculated peak shapes is an integral part of the procedure.

Complex Formation and Electrophoretic Mobility. The common basis of each procedure is the analysis of the changes in the electrophoretic mobility of a protein on complexation with a ligand (L) present in the electrophoresis buffer (Figure 1). The electrophoretic mobility μ ($\text{cm}^2 \text{V}^{-1} \text{s}^{-1}$) of a protein induced by a voltage gradient along the capillary is related to the net charge of the protein and to the inverse of its mass (eq 1). A number of



functional forms have been empirically determined to approximate these relationships:⁷ one is $\mu \simeq z / (m^{2/3})$. Knowledge of the exact form is not necessary for ACE, so long as it does not change as a function of ligand or protein concentration. When a protein forms a complex with a charged ligand of relatively small mass, the change in the electrophoretic mobility of the protein-ligand complex resulting from the change in charge is large, while the contribution to the change in electrophoretic mobility due to the change in mass is negligible (eq 1). The protein-ligand complex may then have a measurable difference in electrophoretic mobility relative to the free protein.⁸ Scatchard analysis of the change in the electrophoretic mobility of the protein as a function of the concentration of the ligand in the electrophoresis buffer allows the determination of the binding constant (K_b) for the interaction.³

Interaction of a protein and a ligand that induces a change in the migration time of the protein may also broaden the peak due to the protein in the region of concentrations corresponding to migration times intermediate between that of free protein and that of its saturated complex with ligand (Figure 1). This broadening is most pronounced if the dissociation time ($1/k_{off}$) is of the same magnitude as the migration time of the protein.

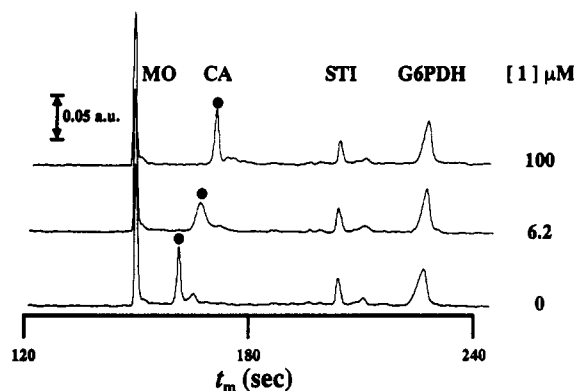


Figure 1. Electrophoresis of a mixture of carbonic anhydrase (●), mesityl oxide (MO), soybean trypsin inhibitor (STI), and glucose-6-phosphate dehydrogenase (G6PDH) in buffer consisting of glycine (192 mM), Tris (25 mM), and various concentrations of ligand 1. The variations in absolute migration times t_m of the noninteracting markers are <2%. The total length of the capillary was 70 cm (45 cm from injection to detection).

Analysis of this broadening makes it possible to estimate values for k_{off} and k_{on} in certain cases.

We chose CA from bovine erythrocytes as the protein for this study for several reasons. The CA does not adsorb to the wall of the capillary under our experimental conditions.³ The protein is commercially available and inexpensive. The mechanism of its action is well-characterized.⁹ The reaction it catalyzes—the hydration of carbon dioxide—is medically important.⁹ The specific inhibition of CA in the eye has been exploited in the development of new antiglaucoma agents.¹⁰ The single-crystal X-ray structure of the carbonic anhydrase has been carried out at 2.0-Å resolution.¹¹ A broad range of arylsulfonamides inhibit the enzyme.⁹ The binding of arylsulfonamides to the active site of the enzyme is well-understood:^{9,12} the active site is a cavity, approximately 15 Å deep and 15 Å wide. The dissociation constants of complexes of arylsulfonamides and CA range from 10^{-6} to 10^{-9} M.⁹

We^{3,13} and others^{14–17} have demonstrated changes in mobility of receptors on binding of ligand under conditions of CE. Binding interactions between vancomycin and peptides,^{13,15} between enzyme and cofactors,³ and between lectins and sugars¹⁴ have been quantified using CE. Changes in electrophoretic mobilities of two calcium binding proteins, parvalbumin and calmodulin, upon binding calcium present in the electrophoresis buffer have been demonstrated¹⁶ and subsequently quantified.³ Binding of ethidium bromide, a positively charged intercalating agent, to DNA restriction fragments in a polyacrylamide gel-filled electrophoresis capillary resulted in an increase in migration time.¹⁷ Affinity methods have also been developed using tube and slab gel electrophoresis.^{5,18}

Results and Discussion

Capillary Electrophoresis of CA. The sample CA was dissolved in electrophoresis buffer (pH 8.3) consisting of glycine (192 mM) and Tris (25 mM). This CA sample solution also contained mesityl oxide (MO) as neutral marker (to measure the rate of electroosmotic flow in the capillary) and at least one of the following as noninteracting protein markers: horse heart myoglobin (HHM), glucose-6-phosphate dehydrogenase (G6PDH) from *Leuconostoc mesenteroides*, and soybean trypsin inhibitor (STI). The capillary was equilibrated with electrophoresis buffer

consisting of the same glycine-Tris buffer and known concentrations of the charged ligand 1. The initial exposure of the enzyme to the ligand(s) occurred on introduction of the CA into the preequilibrated capillary. In the case of the competition experiment to determine the binding constant of a neutral ligand relative to the charged ligand 1, the electrophoresis buffer contained known concentrations of the two ligands. The electropherograms obtained using different concentrations of ligand(s) in the electrophoresis buffer were analyzed for changes in the migration time t_m of CA as a function of the ligand concentration(s). Scatchard analysis allowed the measurement of the binding constant for the interaction of the ligand with CA. The migration times and peak widths of the neutral (MO) and protein markers (HHM, G6PDH, STI) were essentially invariant in each set of experiments. The same series of electropherograms were analyzed by comparing with electropherograms generated by simulation using different values for k_{on} and k_{off} as input parameters.

In this study, we synthesized a low molecular weight arylsulfonamide ligand 1 designed to bear a charge of -3 at the pH of the electrophoresis buffer (Scheme 1). The three key elements in the structure of the charged ligand 1 are: a sulfonamide group, the moiety that is recognized by CA; a tail group composed of three carboxylate groups constructed on a tris(hydroxymethyl)aminomethane core which gives ligand 1 a net charge of -3 at pH 8.3; and an adipate spacer arm. The three sections of the charged ligand were conveniently assembled using amide bond-forming reactions (Scheme 1).

Scatchard Analysis of CA Interacting with a Charged Ligand (L_{\pm}). Figure 2a presents an expanded set of experimental electropherograms showing the change in the migration time and peak shape of the CA peak with increasing concentration of charged ligand 1 in the electrophoresis buffer. The basis for using Stachard analysis to determine the binding constant (K_b^{\pm}) of charged ligand 1 to CA from this set of electropherograms is summarized in eqs 2–5. The assumptions¹⁹ associated

$$K_b^{\pm} = [CA \cdot L_{\pm}] / [CA][L_{\pm}] \quad (2)$$

$$\delta \Delta t_{m,[L_{\pm}]} = \Delta t_{m,[L_{\pm}]} - \Delta t_{m,[L_{\pm}]=0} \quad (3)$$

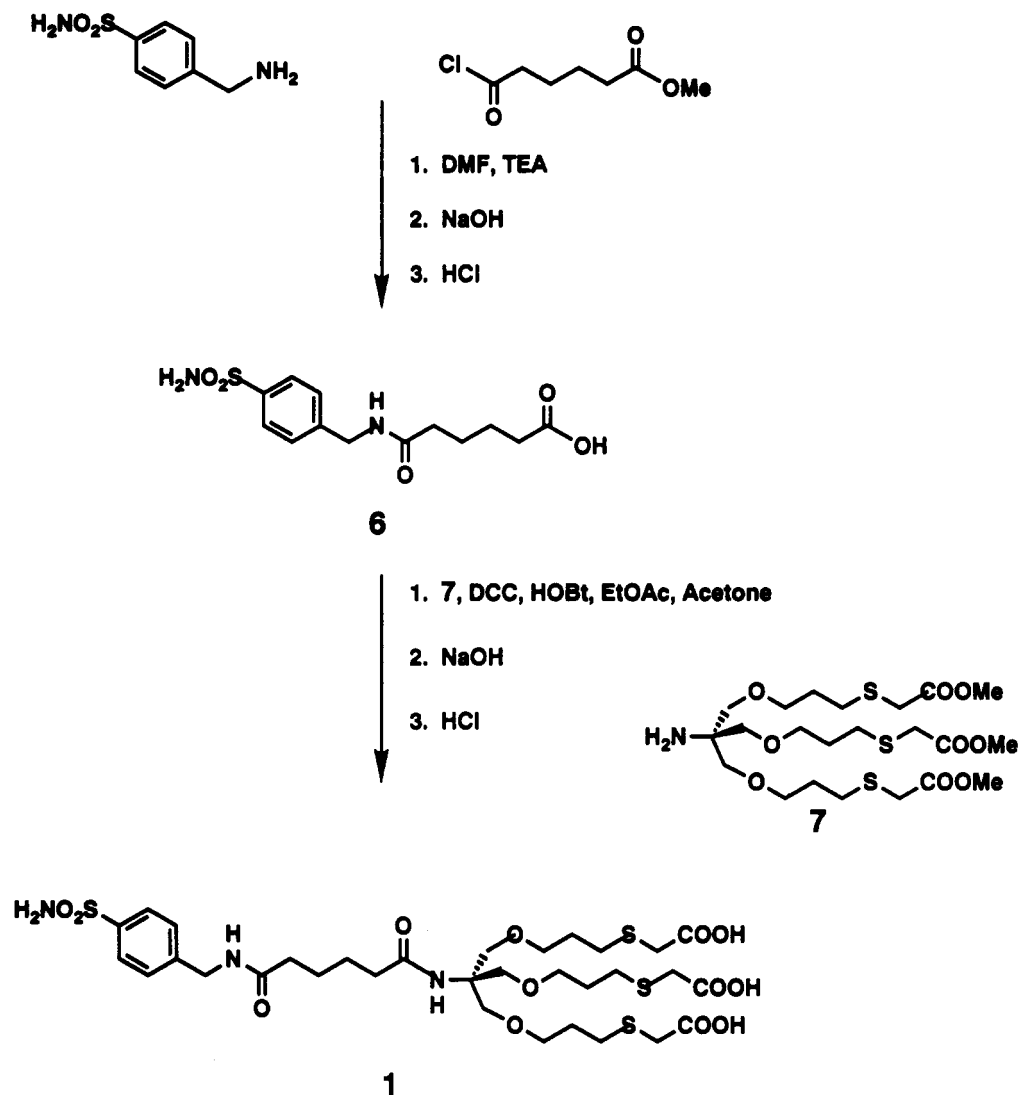
$$R_f = \delta \Delta t_{m,[L_{\pm}]} / \delta \Delta t_{m,max} \\ = [CA \cdot L_{\pm}] / ([CA] + [CA \cdot L_{\pm}]) \quad (4)$$

$$R_f = K_b^{\pm} [L_{\pm}] / (1 + K_b^{\pm} [L_{\pm}]) \quad (5)$$

$$R_f / [L_{\pm}] = K_b^{\pm} - K_b^{\pm} R_f \quad (6)$$

with the use of eq 2–5 for analyzing the interaction of CA with ligand 1 include the following: (a) the interaction between the ligand and the CA molecule is monovalent, (b) the amount of CA is much lower than the total amount of ligand available for binding, and (c) that equilibrium is achieved during the electrophoretic run. An added assumption, unique to ACE, is that the interaction of the ligand and the CA with the capillary wall does not significantly alter the binding interaction of the CA with the ligand. This assumption is *not* that the CA does not associate with the capillary wall, only that the extent of any association is the same with CA and with $CA \cdot L_{\pm}$, and

Scheme I



that this association is independent of the concentration of L_{\pm} in the buffer.

Here $\delta\Delta t_{m,[L_{\pm}]}$ is the change in the migration time due to the presence of the ligand in the electrophoresis buffer²⁰ and $\Delta\delta t_{m,\max}$ is the value of $\delta\Delta t_m$ at saturating concentrations of charged ligand L_{\pm} . The ratio R_f also gives the averaged fraction of the CA sites occupied by the ligand. Eq 6 gives a convenient linearized form appropriate for Scatchard analysis. For the set of data presented in Figure 2a, the binding constant K_b^{\pm} obtained using eq 6 was $1.5 \times 10^5 \text{ M}^{-1}$ ($r > 0.98$). The dissociation constant $K_d^{\pm} = (1/K_b^{\pm})$, which is the concentration of the charged ligand 1 that causes the migration time of CA to change by half the maximum attainable change ($\delta\Delta t_{m,\max}$), was found to be $7 \mu\text{M}$.

Scatchard Analysis of Competitive Binding of Electrically Neutral (L_0) and Charged Ligands (L_{\pm}) to CA. Direct analysis of the interaction of CA with electrically neutral, low molecular weight ligands (L_0) using ACE is not possible because the electrophoretic mobilities of CA and $\text{CA}\cdot L_0$ complex are relatively similar. The neutral ligand L_0 does not introduce a change in charge of the protein-ligand complex, and complex formation results in an undetectable increase in the mass. Thus, the analysis outlined in the preceding section is not directly applicable.

One way of estimating the binding constant (K_b^0) of a neutral ligand L_0 is to allow it to compete with a charged ligand L_{\pm} of known binding constant K_b^{\pm} . Figure 3a shows a set of electropherograms for CA in an electrophoresis buffer containing a fixed concentration ($50 \mu\text{M}$) of ligand 1 and increasing concentration (0 – $100 \mu\text{M}$) of ligand 2. The binding constant for the electrically neutral ligand 2 can then be determined by Scatchard analysis (eqs 7–10) following a procedure analogous to that used for the

$$K_b^0 = [\text{CA}\cdot L_0]/[\text{CA}][L_0] \quad (7)$$

$$R_f = \delta\Delta t_{m,[L_0]}/\delta\Delta t_{m,\max} = [\text{CA}\cdot L_0]/([\text{CA}] + [\text{CA}\cdot L_0] + [\text{CA}\cdot L_{\pm}]) \quad (8)$$

$$R_f = (K_b^0[L_0]/(1 + (K_b^0[L_0] + (K_b^{\pm}[L_{\pm}])) \quad (9)$$

$$R_f/[L_0] = (K_b^0) - (K_b^0)R_f \quad (10)$$

$$K_b^0 = K_b^0/(1 + K_b^{\pm}[L_{\pm}]) \quad (11)$$

charged ligand alone. In this case the change in the migration time ($\delta\Delta t_m$) is measured relative to the migration of CA in the presence of the electrophoresis buffer of an initial, fixed concentration of the charged ligand 1 alone.

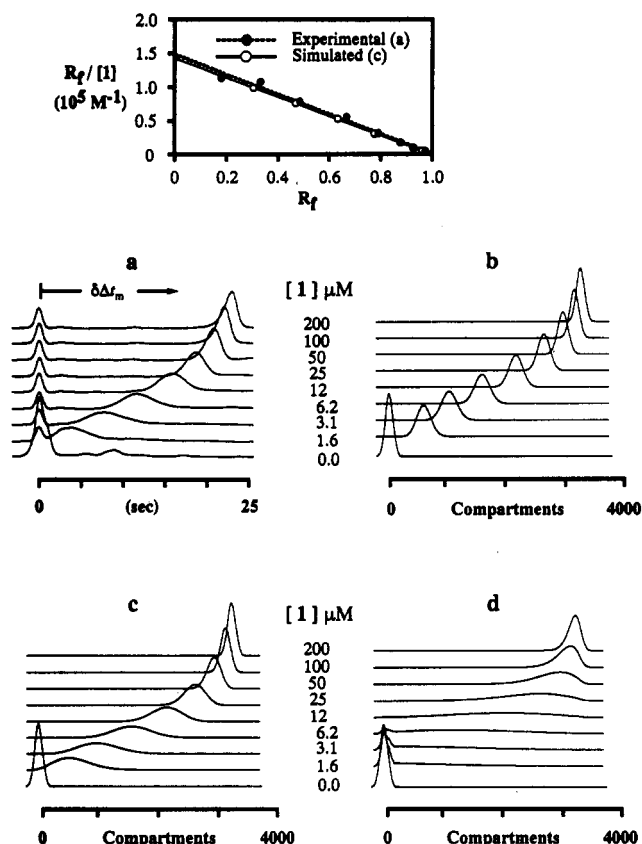
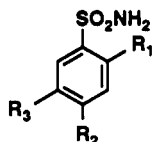


Figure 2. The migration time of CA changes with increasing concentration of charged ligand 1 in the electrophoresis buffer. The nonmobile peak is due to horse heart myoglobin. Stacked electropherograms a were obtained experimentally ($[CA]_0 = 10 \mu\text{M}$; 192 mM glycine–25 mM Tris buffer, pH 8.3) and b–d were generated by simulation. Simulation parameters: (b) $k_{\text{off}} = 1.0 \text{ s}^{-1}$; $k_{\text{on}} = 1.5 \times 10^5 \text{ M}^{-1} \text{ s}^{-1}$; (c) $k_{\text{off}} = 0.1 \text{ s}^{-1}$; $k_{\text{on}} = 1.5 \times 10^4 \text{ M}^{-1} \text{ s}^{-1}$; (d) $k_{\text{off}} = 0.01 \text{ s}^{-1}$; $k_{\text{on}} = 1.5 \times 10^3 \text{ M}^{-1} \text{ s}^{-1}$. In the simulation, the concentration in each compartment was adjusted every 10 ms and the contents of the compartments for the mobile complex was transferred every 100 ms. The graph is a Scatchard plot of the experimental data a and simulation data c using eq 6.



	R ₁	R ₂	R ₃
2	H	H	H
3	H	CH ₃	H
4	Cl	Cl	Cl
5	H	NO ₂	H

Eq 8 is analogous to eq 4 and eq 10 to eq 6. The term K_b° is the apparent binding constant of the neutral sulfonamide in the presence of the charged ligand. Eq 11 gives the relationship between the apparent (K_b°) and actual (K_b°) binding constants for the neutral ligand where K_b^{\pm} and $[L_{\pm}]$ are the binding constant and fixed concentration of the charged ligand in the electrophoresis buffer, respectively. For the data presented in Figure 3a, the apparent binding constant K_b° of the neutral ligand 2 in the presence of the charged ligand 1 using eq 10 was $1.3 \times 10^5 \text{ M}^{-1}$ ($r > 0.99$). The actual binding constant $K_b^{\circ} = 1.1 \times 10^6 \text{ M}^{-1}$ was obtained using eq 11 and the values 1.5

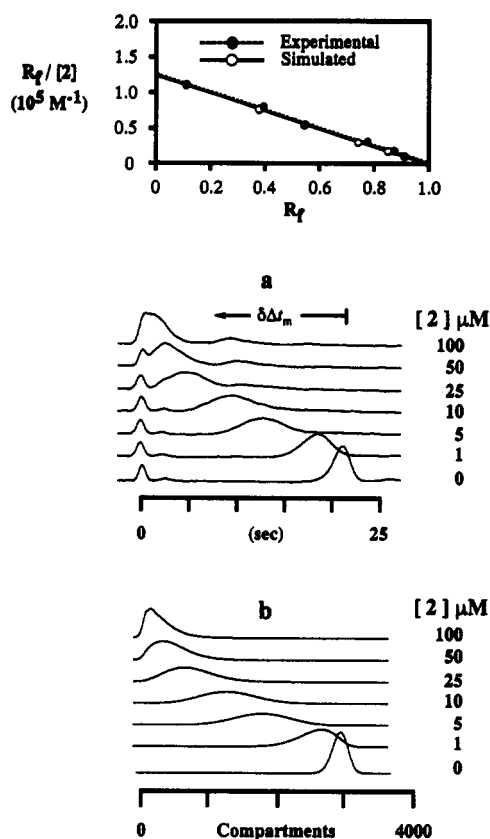


Figure 3. The migration time of CA changes with increasing concentration of neutral ligand 2 in the presence of 50 μM of charged ligand 1 in the electrophoresis buffer. The nonmobile peak is due to horse heart myoglobin. Stacked electropherograms a were obtained experimentally ($[CA]_0 = 10 \mu\text{M}$; 192 mM glycine–25 mM Tris buffer, pH 8.3) and b were generated by simulation using the parameters $k_{\text{off}} = 0.1 \text{ s}^{-1}$ and $k_{\text{on}} = 1.1 \times 10^5 \text{ M}^{-1} \text{ s}^{-1}$ for the neutral ligand. CA·L₀ is not mobile within the reference frame. The remainder of the simulation parameters were similar to Figure 2c. The graph is a Scatchard plot of the data using eq 10.

Table I. Binding Constants of Ligands 2–5 to Bovine CA-B Obtained by ACE

ligand	ACE ^a (10^6 M^{-1})	literature ^b (10^6 M^{-1})	literature ^c (10^6 M^{-1})
2	1.1	0.3	0.7
3	1.9	0.7	2.0
4	4.5	–	6.8
5	7.0	2.6	16

^a The concentration of the charged ligand 1 was 50 μM . ^b Literature values are for bovine CA-B measured at 25 °C in 0.1 M Tris-HCl buffer (pH 7.2) and are taken from ref 23. ^c Literature values are for human CA-C measured at 25 °C in 0.02 M phosphate buffer (pH 6.5) and are taken from ref 24.

$\times 10^5 \text{ M}^{-1}$ and 50 μM for K_b^{\pm} and $[L_{\pm}]$, respectively. Table I shows the binding constants K_b° of a number of neutral sulfonamides to bovine CA obtained using this competition procedure. For comparison, Table I also shows the binding affinity of the same set of ligands reported for bovine²¹ and human CA.²²

Simulation of CA Interacting with a Charged Ligand (L_{\pm}). Figure 2a shows that the migration time of the CA changes with the concentration of L_{\pm} . The peak for CA also broadens in the region of intermediate migration time. This type of broadening has been observed previously in many forms of chromatography,²⁵ and reflects equilibration between species with different migration times (in this instance, free protein and protein–ligand

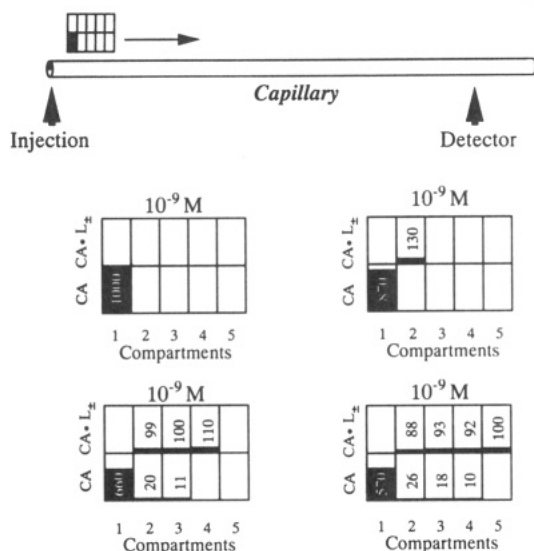


Figure 4. The simulation continuously adjusts the contents of each compartment of the reference frame as the frame travels through the capillary. For simplicity, the propagation of the contents of a single compartment is shown. The elapsed time (ms) in the series of frames are (a) 0, (b) 100, (c) 300, and (d) 400.

complex) occurring with rates comparable to the time required for the electrophoresis experiment. To extract these rate constants for the peak widths, we simulated the behavior of CA under conditions of the ACE experiment.

The model²⁶⁻²⁸ we used to analyze the migration of CA in an electrophoresis buffer containing ligand assumed a reference frame that traveled along the capillary at the velocity of the free CA (Figure 4). The origin of the reference frame was designated as the position of migration of CA without bound ligand in the electrophoresis buffer. The terminus of the reference frame was set as the position of the maximum displacement.²⁹ This latter condition is satisfied at saturating concentrations of the ligand in the electrophoresis buffer. Thus, the CA-ligand complex was mobile within this reference frame, and its velocity within the frame was determined from the difference in the migration times of CA with no ligand in the electrophoresis buffer and with saturating concentration of the ligand.

The reference frame was subdivided into two linear arrays of compartments: one array represented the compartments for the free CA and the other for the CA·L_± complex. The unbound CA was introduced in a Gaussian distribution into the compartments reserved for free CA centered on the origin of the reference frame. The width of the Gaussian distribution was adjusted to match the peak width of CA in the electropherogram obtained in the absence of ligand in the buffer. As in the actual experiment, CA was introduced in the compartments as free CA and did not interact with the ligand until the simulation was initiated.

The main element of the simulation was a continuous iteration cycle that consisted of two steps: an equilibration step and a translation step. Figure 4 shows the early steps of the simulation for the propagation of the contents a plug of CA initially occupying a single compartment. The equilibration step involved periodic adjustment ($\Delta t = 1-10$ ms)³⁰ of the concentrations of the free and complexed proteins in every set of paired compartments (eqs 12-14). The term $\Delta[\text{CA}]_{x,\Delta t}$ in eq 12 represents the net change in concentration of CA in x th paired compartments over the time interval Δt . To simplify the simulation, the rate of

formation of the CA-ligand complex (eq 12) was approximated using first-order kinetics by assuming a steady state concentration for the ligand (L_{\pm}) equal to its initial concentration in the electrophoresis buffer. Eqs 13 and 14 update the concentration in each compartment to reflect the new concentrations of CA and CA·L_± after a time interval of Δt using the value obtained from eq 12.

$$\Delta[\text{CA}]_{x,\Delta t} = k_{\text{off}}[\text{CA}\cdot\text{L}_{\pm}]_{x,t}\Delta t - k_{\text{on}}[\text{CA}]_{x,t}[\text{L}_{\pm}]\Delta t \quad (12)$$

$$[\text{CA}]_{x,t+\Delta t} = [\text{CA}]_{x,t} + \Delta[\text{CA}]_{x,\Delta t} \quad (13)$$

$$[\text{CA}\cdot\text{L}_{\pm}]_{x,t+\Delta t} = [\text{CA}\cdot\text{L}_{\pm}]_{x,t} - \Delta[\text{CA}]_{x,\Delta t} \quad (14)$$

The content of the x th compartment for CA·L_± complex was periodically shifted to the $(x + 1)$ th compartment every time interval (100 ms) equivalent to the time required by the CA·L_± complex to travel the width of the compartment of the reference frame under the conditions of electrophoresis.²⁹ This translation step stimulated the fact that the CA·L_± was mobile within the reference frame; the free CA remained immobile in the reference frame by definition.

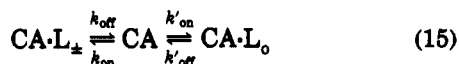
The simulation was terminated when the total time for the simulation equaled the experimentally determined migration time (t_m) for the CA in the electrophoresis buffer without ligand. The contents of each pair of compartments (CA and CA·L_±) were summed and then plotted versus distance from the origin of the moving reference frame to provide the distribution of the CA at different positions of the reference frame. This distribution provided a "snapshot" approximation of the experimental electropherogram. We assumed that the experimental electropherogram was a real-time record of the UV absorbance due to the protein as the hypothetical reference frame moved past the detector.

We carried out a number of simulations to approximate the experimental electropherograms (Figure 2a) by using different combinations of k_{on} and k_{off} for eq 12. Figures 2b-d are three of the simulation-generated electropherograms. The search for the correct combination of k_{on} and k_{off} to use in the simulation was limited to combinations that gave a binding constant equal to the binding constant obtained experimentally. Scatchard analysis of the simulation-generated electropherograms (Figure 2c) using eq 6 gave a K_D^{\pm} of $1.5 \times 10^5 \text{ M}^{-1}$ ($r > 0.99$).³¹

An important finding from the simulation was that only one set of the simulation-generated electropherograms (Figure 2c) approximated the peak widths of the experimental electropherogram (Figure 2a). The values of k_{off} (0.1 s^{-1}) and k_{on} ($1.5 \times 10^4 \text{ M}^{-1} \text{ s}^{-1}$) used to generate Figure 2c fall within the range of values of k_{off} ($0.05-0.5 \text{ s}^{-1}$) and k_{on} ($10^4-10^6 \text{ M}^{-1} \text{ s}^{-1}$) reported for a number of aryl-sulfonamides.^{22b,24} The increase in the peak width did not result from the extra time the CA spent in the capillary.³² In fact, the CA peak sharpens at saturating concentrations of the charged ligand despite having longer migration time.

Simulation of CA Interacting with One Charged (L_±) and One Neutral (L₀) Ligands. The model we used can be readily extended to simulate the migration of CA in the capillary while interacting simultaneously with two or more ligands. For the case of CA interacting with two ligands: L_± (charged ligand) and L₀ (neutral ligand), a third linear array of compartments was added to the

reference frame to contain the $CA \cdot L_o$ complex. This variation assumed that the interconversion between $CA \cdot L_{\pm}$ and $CA \cdot L_o$ had to proceed through free CA (eq 15).



Thus, the equilibration step of the simulation was expanded to compute the amounts of $CA \cdot L_{\pm}$ and $CA \cdot L_o$ alternately using eqs 12–14. The translation step shifted only the contents of the compartments for $CA \cdot L_{\pm}$ because the $CA \cdot L_{\pm}$ complex was mobile within the reference frame ($\mu_{CA} \neq \mu_{CA \cdot L_{\pm}}$) and the free CA and the $CA \cdot L_o$ complex were immobile ($\mu_{CA} \approx \mu_{CA \cdot L_o}$). The rest of the simulation was basically the same.

Figure 3b shows the electropherograms predicted by the model for the migration of CA in an electrophoresis buffer containing 50 μ M of charged ligand 1 and increasing amounts of neutral ligand 2. The binding constants K_b^{\pm} and K_b^o used as input parameters in the simulation were $1.5 \times 10^5 \text{ M}^{-1}$ and $1.1 \times 10^6 \text{ M}^{-1}$, respectively. Scatchard analysis of the simulation-generated electropherograms (Figure 3b) using eq 10 did not return the original value of the binding constant used in the simulation but instead gave a value of $1.3 \times 10^5 \text{ M}^{-1}$ ($r > 0.99$); this value was equal to the apparent K_b^o measured experimentally (Figure 3a). The original value of the binding constant (K_b^o) used in the simulation was obtained using eq 11.

Conclusion

ACE is a useful method to study protein–ligand interactions. The attractive features of ACE include its ability to provide assessment of protein–ligand interactions using very small amounts of samples and ligands in relatively short time. ACE relies only on the migration time and shape of the peak and not on its area. The concentration of the protein in the sample does not appear in the equations used for Scatchard analysis (eqs 6 and 10). The protein need not be pure; simultaneous determination of individual binding constants using a sample of a mixture of isozymes or different proteins is possible.³ In this study, ACE allowed simultaneous measurement of the binding constant of 1 to CA, through changes in migration time and of the *off* rate for the binding interaction from the peak width.³³

A major consideration in using ACE remains the tendency of proteins to adsorb on the wall of uncoated capillaries; this tendency becomes more pronounced when the pH of the electrophoresis buffer is close to or lower than the pI of the protein. A number of approaches are available to control this interaction between protein and capillary wall including the use of additives to the buffer and chemical modification of the silanol groups of the capillary wall.³⁴ ACE requires that at least one of the ligands should have a sufficient charge to cause a measurable change in the migration time of the protein–ligand complex.

The simulation suggests that the electropherograms resulting from protein–ligand interaction can be explained in terms of relatively few variables: *on* and *off* rates (and thus, binding constant), concentration of the ligand(s), and the relative mobilities of the protein and the protein–ligand complex(es).²⁸ The simulation also suggests that quantitative determination of high binding constants (associated with slow dissociation of the ligand from the

protein) can be achieved by increasing the residence time of the protein in the capillary to allow for equilibration to take place. This will also require adjusting the amount of protein so that it is lower than the amount of ligand available for binding.¹⁹ Qualitative screening of strong binding ligands can be undertaken using shorter run times; the expected electropherograms will resemble Figure 2d. For weak protein–ligand interactions, high background absorbance and changes in buffer properties due to the ligand should be anticipated at the high concentration of ligand required to influence the mobility of the protein.³⁵

Experimental Section

Apparatus. The ISCO 3140 capillary electrophoresis apparatus (ISCO, Inc., Lincoln, NE) was used in this study with the anode on the injection side and the cathode on the detection side. The capillary tubing (Polymicro Technologies, Inc., Phoenix, AZ) was of uncoated fused silica with an internal diameter of 50 μ m and a total length of 100 cm (75 cm from the injection side to the detector) unless stated otherwise. The elution was monitored on-column at 200 nm. The temperature of the column was maintained at 30 ± 1 °C. The electropherogram raw data were collected using ICE software (ISCO, Inc., Lincoln, NE) and later exported as ASCII files for processing and analysis using Kaleidagraph (Synergy Software, Reading, PA).

Simulation. The simulation programs were written in PASCAL. The reference frame was constructed by dividing the frame into two arrays of compartments parallel to the direction of travel. The width of the compartments corresponds to the distance that the protein–ligand complex would have traveled in the reference frame using experimentally determined velocities for the free and the complexed CA. The concentration in each paired compartment was iteratively adjusted every 1–10 ms using eqs 12–14. The concentration of the ligand was assumed constant and equal to the concentration in the electrophoresis buffer. The concentration of the complexed CA in the *x*th compartment was transferred to the (*x* + 1)th compartment every 100 ms. The simulation generated data were also analyzed and plotted using Kaleidagraph.

Chemicals. Bovine carbonic anhydrase B (EC 4.2.1.1), glucose 6-phosphate dehydrogenase (*Leuconostoc mesenteroides*, EC 1.1.1.49) and soybean trypsin inhibitor were purchased from Sigma. Horse heart myoglobin was purchased from U.S. Biochemical Corp. Stock solutions (1 mg/mL) of bovine carbonic anhydrase, horse heart myoglobin, glucose-6-phosphate dehydrogenase, and soybean trypsin inhibitor were each prepared by dissolving the lyophilized proteins in glycine (192 mM) and Tris (25 mM) buffer. Benzenesulfonamide, 4-toluenesulfonamide, and 4-nitrobenzenesulfonamide were purchased from Aldrich. 2,4,5-trichlorobenzenesulfonamide was prepared from 2,4,5-trichlorobenzenesulfonyl chloride (TCI-America) and recrystallized from 95% ethanol, mp 187–189 °C.³⁶

Procedures. Eight nanoliters of a sample solution containing 0.3 mg/mL of CA and 0.3 mg/mL of each of the noninteracting protein markers and mesityl oxide (neutral marker) in 192 mM glycine–25 mM Tris buffer (pH 8.3) was introduced into the capillary by vacuum injection. The electrophoresis was carried out using an electrophoresis buffer (pH 8.3) consisting of 192 mM glycine, 25 mM Tris, and appropriate concentrations (0–200 μ M) of arylsulfonamide ligand(s). The electrophoresis was carried out under constant voltage of 30 kV generating a current of approximately 10 μ A.

Preparation of 6. To a solution of 4-(aminomethyl)benzenesulfonamide hydrochloride (10.0 g, 45 mmol) and triethylamine (9.0 g, 89 mmol) in dimethylformamide (150 mL) at 0 °C was added methyl adipoyl chloride (8.0 g, 45 mmol). The mixture was stirred at 0 °C for 1 h and then at room temperature for 6 h. The solution was filtered and concentrated *in vacuo*. Flash chromatography on silica gel (chloroform–methanol, 9:1) afforded the methyl ester of 6 as a solid (14.0 g, 95%). The product was recrystallized from a mixture of chloroform and methanol to yield planar crystals: mp 124–125 °C; ¹H NMR (400 MHz, DMSO-*d*₆) δ 8.43 (t, *J* = 5.9 Hz, 1 H, NH), 7.77 (d, *J* = 8.3 Hz, 2 H, aryl H), 7.41 (d, *J* = 8.3 Hz, 2 H, aryl H), 7.33 (s, 2 H,

SO_2NH_2), 4.32 (d, $J = 5.9$ Hz, 2 H, ArCH_2N), 3.58 (s, 3 H, OCH_3), 2.32 (t, $J = 6.9$ Hz, 2 H, $\text{CH}_2\text{CH}_2\text{CO}_2\text{CH}_3$), 2.17 (t, $J = 6.9$ Hz, 2 H, $\text{CH}_2\text{CH}_2\text{CONH}$), 1.53 (m, 4 H, CH_2CH_2); ^{13}C NMR (100.6 MHz, $\text{DMSO}-d_6$) δ 173.4, 172.2, 143.9, 142.6, 127.5, 125.8, 51.3, 41.7, 35.0, 33.1, 24.8, 24.1; HRMS (FAB) m/e 329.1181 ($\text{M} + \text{H}$) $^+$, calcd for $\text{C}_{14}\text{H}_{21}\text{N}_2\text{O}_5\text{S}$ 329.1171.

To a solution of sodium hydroxide (0.1 N, 200 mL) was added the methyl ester of **6** (4.0 g, 12.2 mmol). The solution was stirred at room temperature for 7 h and then acidified with concentrated HCl to pH \sim 3. The resulting precipitate **6** was filtered, washed with acidic water, and air-dried. This solid was recrystallized from acidic water to yield white needles (3.5 g, 92%): mp 121–122 $^\circ\text{C}$; ^1H NMR (400 MHz, $\text{DMSO}-d_6$) δ 8.42 (t, $J = 5.9$ Hz, 1 H, NH), 7.76 (d, $J = 8.3$ Hz, 2 H, aryl H), 7.40 (d, $J = 8.3$ Hz, 2 H, aryl H), 7.31 (s, 2 H, SO_2NH_2), 4.31 (d, $J = 5.9$ Hz, 2 H, ArCH_2N), 2.22 (t, $J = 7.0$ Hz, 2 H, $\text{CH}_2\text{CH}_2\text{CO}_2\text{H}$), 2.16 (t, $J = 7.0$ Hz, 2 H, $\text{CH}_2\text{CH}_2\text{CONH}$), 1.52 (m, 4 H, CH_2CH_2); ^{13}C NMR (100.6 MHz, $\text{DMSO}-d_6$) δ 174.4, 172.1, 143.9, 142.5, 127.4, 125.7, 41.7, 35.0, 33.4, 24.8, 24.2; HRMS (FAB) m/e 315.1005 ($\text{M} + \text{H}$) $^+$, calcd for $\text{C}_{13}\text{H}_{19}\text{N}_2\text{O}_5\text{S}$ 315.1015.

Preparation of Trimethyl Ester of 1. To an ethyl acetate solution (10 mL) of the Boc-protected tris(trimethyl) ester **7**³⁷ (1.0 g, 1.5 mmol) was added trifluoroacetic acid (0.6 mL, 7.5 mmol). The solution was stirred at room temperature for 2 h. The reaction mixture was diluted with ethyl acetate, washed with 20% aqueous sodium bicarbonate, water, and saturated sodium chloride, respectively. The organic layer was dried using anhydrous magnesium sulfate and concentrated in vacuo. The product, isolated as the free amine (0.52 g, 61%), was used directly for the next coupling reaction. To a solution of amine **7** (0.52 g, 0.93 mmol) in ethyl acetate (20 mL) and **6** (0.29 g, 0.92 mmol) in acetone (15 mL) at 0 $^\circ\text{C}$ was added dicyclohexylcarbodiimide (0.21 g, 1.01 mmol) and 1-hydroxybenzotriazole (0.14 g, 0.92 mmol). After mixing, the reaction was allowed to warm to room temperature and stirred for 24 h. The solution was filtered and concentrated in vacuo. Flash chromatography on silica gel (chloroform–methanol, 20:1) afforded the desired product as a yellow oil (0.70 g, 89%): ^1H NMR (400 MHz, $\text{DMSO}-d_6$) δ 8.38 (t, $J = 5.9$ Hz, 1 H, NH), 7.76 (d, $J = 8.3$ Hz, 2 H, aryl H), 7.40 (d, $J = 8.3$ Hz, 2 H, aryl H), 7.32 (s, 2 H, SO_2NH_2), 7.06 (s, 1 H, NH), 4.31 (d, $J = 5.8$ Hz, 2 H, ArCH_2N), 3.63 (s, 9 H, $(\text{CO}_2\text{CH}_3)_3$), 3.54 (s, 6 H, $\text{C}(\text{CH}_2\text{O})_3$), 3.44 (t, $J = 5.5$ Hz, 6 H, $(\text{OCH}_2\text{CH}_2)_3$), 3.33 (s, 6 H, $\text{SCH}_2\text{CO}_2\text{CH}_3$), 2.60 (t, $J = 7.2$ Hz, 6 H, $(\text{OCH}_2\text{CH}_2\text{CH}_2\text{S})_3$), 2.13 (t, $J = 6.9$ Hz, 2 H, $\text{CH}_2\text{C}(=\text{O})\text{NH}$), 2.07 (t, $J = 6.9$ Hz, 2 H, $\text{CH}_2\text{C}(=\text{O})\text{NH}$), 1.72 (m, 6 H, $(\text{OCH}_2\text{CH}_2\text{CH}_2\text{S})_3$), 1.47 (m, 4 H, $\text{CH}_2\text{CH}_2\text{CH}_2\text{C}(=\text{O})\text{NH}$); ^{13}C NMR (100.6 MHz, $\text{DMSO}-d_6$) δ 172.3, 172.1, 170.7, 143.8, 142.5, 127.4, 125.6, 69.0, 68.0, 59.6, 52.0, 48.6, 41.6, 35.6, 35.2, 32.6, 28.6, 25.1, 24.9; HRMS (FAB) m/e 878.2679 ($\text{M} + \text{Na}$) $^+$, calcd for $\text{C}_{85}\text{H}_{57}\text{N}_3\text{O}_{13}\text{S}_4\text{Na}$ 878.2672.

Preparation of Ligand 1. To a methanol solution (5 mL) of the trimethyl ester of **1** (0.5 g, 0.6 mmol) was added 1 N sodium hydroxide (5 mL, 5 mmol). The reaction was carried out at room temperature and monitored by TLC (chloroform–methanol = 9:1, v/v). The hydrolysis of the triester was completed after one day. Dowex 50W-X8 (H^+ form, 20–50 mesh) resin was added to the solution that its pH was 3.5. The solution was stirred at room temperature for 2 h, and acidity of the solution was monitored using pH indicator strips. The desired product **1** obtained following filtration and concentration in vacuo was isolated as a yellow oil (free acid form; 0.4 g, 84%): ^1H NMR (400 MHz, $\text{DMSO}-d_6$) δ 8.38 (t, $J = 5.9$ Hz, 1 H, NH), 7.76 (d, $J = 8.3$ Hz, 2 H, aryl H), 7.40 (d, $J = 8.3$ Hz, 2 H, aryl H), 7.32 (s, 2 H, SO_2NH_2), 7.06 (s, 1 H, NH), 4.31 (d, $J = 5.9$ Hz, 2 H, ArCH_2N), 3.54 (s, 6 H, $\text{C}(\text{CH}_2\text{O})_3$), 3.41 (t, $J = 6.1$ Hz, 6 H, $(\text{OCH}_2\text{CH}_2\text{CH}_2\text{S})_3$), 3.21 (s, 6 H, $(\text{SCH}_2\text{CO}_2\text{H})_3$), 2.60 (t, $J = 7.2$ Hz, 6 H, $(\text{OCH}_2\text{CH}_2\text{CH}_2\text{S})_3$), 2.14 (t, $J = 7.1$ Hz, 2 H, $\text{CH}_2\text{C}(=\text{O})\text{NH}$), 2.07 (t, $J = 7.1$ Hz, 2 H, $\text{CH}_2\text{C}(=\text{O})\text{NH}$), 1.73 (m, 6 H, $(\text{OCH}_2\text{CH}_2\text{CH}_2\text{S})_3$), 1.48 (m, 4 H, $\text{CH}_2\text{CH}_2\text{CH}_2\text{C}(=\text{O})\text{NH}$); ^{13}C NMR (100.6 MHz, $\text{DMSO}-d_6$) δ 172.4, 172.2, 171.1, 143.9, 142.5, 127.5, 125.7, 69.1, 68.0, 59.6, 41.7, 35.7, 35.2, 33.2, 28.7, 28.6, 25.1, 24.9; HRMS (FAB) m/e 836.2192 ($\text{M} + \text{Na}$) $^+$, calcd for $\text{C}_{32}\text{H}_{51}\text{N}_3\text{O}_{13}\text{S}_4\text{Na}$ 836.2202.

Acknowledgment. We thank Hans A. Biebuyck for helpful discussions and comments about the work. ECB thanks NSF for partial support under a NSF-ROA fellowship.

Supplementary Material Available: Codes (PASCAL) for the simulation of one enzyme–one ligand and one enzyme–two ligands interactions are available (7 pages). Ordering information is given on any current masthead page.

References

- (1) This research was supported by the National Institutes of Health (Grant GM30367), the National Science Foundation (Grant CHE-91-22331 to GMW) and the M.I.T. Biotechnology Processing Engineering Center (Cooperative Agreement CDR-88-03014).
- (2) On leave from Rollins College, Winter Park, FL 1991–1992.
- (3) Chu, Y.-H.; Avila, L. Z.; Biebuyck, H. A.; Whitesides, G. M. Use of Affinity Capillary Electrophoresis To Measure Binding Constants of Ligands to Proteins. *J. Med. Chem.* 1992, 15, 2915–2917.
- (4) Reviews of capillary electrophoresis of proteins: Kuhr, W. G.; Monnig, C. A. Capillary Electrophoresis. *Anal. Chem.* 1992, 64, 389R–407R. Mazzeo, J. R.; Krull, I. S. Coated Capillaries and Additives for the Separation of Proteins by Capillary Zone Electrophoresis and Capillary Isoelectric Focusing. *BioTechniques* 1991, 10, 638–645. Novotny, M. V.; Cobb, K. A.; Liu, J. Recent Advances in Capillary Electrophoresis of Proteins, Peptides, and Amino Acids. *Electrophoresis* 1990, 11, 735–749.
- (5) Reviews of affinity electrophoresis (AE): Takeo, K. Affinity Electrophoresis. In *Advances in Electrophoresis*; Chrambach, A., Dunn, M. J., Radola, B. J., Eds.; BCH Publisher: New York, 1987; Vol. 1 pp 229–279. Lee, M. K.; Lander, A. D. Analysis of Affinity and Structural Selectivity in the Binding of Proteins to Glycosaminoglycans: Development of a Sensitive Electrophoretic Approach. *Proc. Natl. Acad. Sci. U.S.A.* 1991, 88, 2768–2772. Shimura, K. Progress in Affinophoresis. *J. Chromatogr.* 1990, 510, 251–270. Horejsi, V.; Ticha, M. Qualitative and Quantitative Applications of Affinity Electrophoresis for the Study of Protein–Ligand Interactions: A Review. *J. Chromatogr.* 1986, 376, 49–67. Horejsi, V. Affinity Electrophoresis. *Methods Enzymol.* 1984, 104, 275–281. Horejsi, V. Affinity Electrophoresis. *Anal. Biochem.* 1981, 112, 1–8.
- (6) White, R. J.; Philipps, D. Q. Transcriptional Analysis of Multisite Drug–DNA Dissociation Kinetics: Delayed Termination of Transcription by Actinomycin D. *Biochemistry* 1988, 27, 9122–9132. Paton, W. D. M.; Rang, H. P. A Kinetic Approach to the Mechanism of Drug Action. *Adv. Drug. Res.* 1966, 3, 57–80.
- (7) A number of functional forms have been suggested to describe the relationship between electrophoretic mobility and the charge and mass of the protein entity: Compton, B. J.; O'Grady, E. A. Role of Charge Suppression and Ionic Strength in Free Zone Electrophoresis of Proteins. *Anal. Chem.* 1991, 63, 2597–2602. Compton, B. J. Electrophoretic Mobility Modeling of Protein in Free Zone Capillary Electrophoresis and its Application to Monoclonal Antibody Microheterogeneity Analysis. *J. Chromatogr.* 1991, 559, 357–366. Rickard, E. C.; Strohl, M. M.; Nielsen, R. G. Correlation of Electrophoretic Mobilities From Capillary Electrophoresis With Physicochemical Properties of Proteins and Peptides. *Anal. Biochem.* 1991, 197, 197–207. Grossman, P. D.; Colburn, J. C.; Lauer, H. H. A Semiempirical Model for the Electrophoretic Mobilities of Peptides in Free-Solution Capillary Electrophoresis. *Anal. Biochem.* 1989, 179, 28–33. Deyl, Z.; Rohlicek, V.; Adam, M. Separation of Collagens by Capillary Electrophoresis. *J. Chromatogr.* 1989, 480, 371–378.
- (8) Alternatively, a measurable difference in the electrophoretic mobility of the complex may also be achieved by causing an increase in the mass of the complex without proportionately changing the magnitude of its charge, i.e. by using ligands of high molecular weights.
- (9) Reviews: Botre, F.; Gros, G.; Storey, B. T. *Carbonic Anhydrase: From Biochemistry and Genetics to Physiology and Clinical Medicine*; VCH Publishers: New York, 1991. Dodgson, S. J.; Tashian, R. E.; Gros, G.; Carter, N. D. *The Carbonic Anhydrases: Cellular Physiology and Molecular Genetics*; Plenum Press: New York, 1991.
- (10) Baldwin, J. J.; Ponticello, G. S.; Anderson, P. S.; Christy, M. E.; Murcko, M. A.; Randall, W. C.; Schwam, H.; Sugrue, M. F.; Springer, J. P.; Gautheron, P.; Grove, J.; Mallorga, P.; Viader, M.-P.; McKeever, B. M.; Navia, M. A. Thienothiopyran-2-sulfonamides: Novel Topically Active Carbonic Anhydrase Inhibitors for the Treatment of Glaucoma. *J. Med. Chem.* 1989, 32, 2510–2513.
- (11) Eriksson, A. E.; Jones, T. A.; Liljas, A. Refined Structure of Human Carbonic Anhydrase II at 2.0 Å Resolution. *Proteins: Struct. Funct. and Genet.* 1988, 4, 274–282.
- (12) Eriksson, A. E.; Kylsten, P. M.; Jones, T. A.; Liljas, A. Crystallographic Studies of Inhibitor Binding Sites in Human Carbonic Anhydrase II: A Pentacoordinated Binding of the SCN Ion to the Zinc at High pH. *Proteins: Struct. Funct. and Genet.* 1988, 4, 283–293.

- (13) Chu, Y.-H.; Whitesides, G. M. Affinity Capillary Electrophoresis Can Simultaneously Measure Binding Constants of Multiple Peptides to Vancomycin. *J. Org. Chem.* 1992, 57, 3524-3525.
- (14) Honda, S.; Taga, A.; Suzuki, K.; Suzuki, S.; Kakehi, D. Determination of the Association Constant of Monovalent Model Protein-Sugar Interaction By Capillary Zone Electrophoresis. *J. Chromatogr.* 1992, 597, 377-382.
- (15) Carpenter, J. L.; Camilleri, P.; Dhanak, D.; Goddall, D. A Study of the Binding of Vancomycin to Dipeptides using Capillary Electrophoresis. *J. Chem. Soc. Chem. Commun.* 1992, 804-806.
- (16) Kajiwar, H.; Hirano, H.; Oono, K. Binding Shift Assay of Parvalbumin, Calmodulin and Carbonic Anhydrase by High-Performance Capillary Electrophoresis. *J. Biochem. Biophys. Methods* 1991, 22, 263-268.
- (17) Guttman, A.; Cooke, N. Capillary Gel Affinity Electrophoresis of DNA Fragments. *Anal. Chem.* 1991, 63, 2038-2042.
- (18) Chu, Y.-H.; Whitesides, G. M. Unpublished results.
- (19) Horejsi, V. Some Theoretical Aspects of Affinity Electrophoresis. *J. Chromatogr.* 1979, 178, 1-13. Horejsi, V.; Ticha, M. Theory of Affinity Electrophoresis. Evaluation of the Effects of Protein Multivalency, Immobilized Ligand Heterogeneity and Microdistribution and Determination of Effective Concentration of Immobilized Ligand. *J. Chromatogr.* 1981, 216, 43-62.
- (20) To adjust for the effects of the changes in the buffer viscosity and dielectric constant on the electrophoretic mobility of CA, $\Delta t_{m,[L]}$ is the corrected migration time for the protein of interest (CA) relative to a reference protein (horse heart myoglobin in this example).
- (21) The difference in the binding constants are within the limits due to pH.: Kernohan, J. C. A Method for Studying the Kinetics of the Inhibition of Carbonic Anhydrase by Sulphonamides. *Biochim. Biophys. Acta* 1966, 118, 405-412.
- (22) For discussion of inhibition of carbonic anhydrase from different sources by sulfonamides see: (a) Maren, T. H.; Sanyal, G. The Activity of Sulfonamides and Anions Against the Carbonic Anhydrase of Animals, Plants and Bacteria. (b) Maren, T. H. Direct Measurements of the Rate Constants of Sulfonamides With Carbonic Anhydrase. *Mol. Pharmacol.* 1992, 41, 419-426. (c) King, R. W.; Burgen, A. S. V. Kinetic Aspects of Structure-Activity Relations. The Binding of Sulphonamides by Carbonic Anhydrase. *Proc. R. Soc. London, B* 1976, 193, 107-125.
- (23) Carotti, A.; Raguseo, C.; Campagna, F.; Langridge, R.; Klein T. E. Inhibition of Carbonic Anhydrase by Substituted Benzene-sulfonamides. A Reinvestigation by QSAR and Molecular Graphics Analysis. *Quant. Struct.-Act. Relat.* 1989, 8, 1-10.
- (24) Taylor, P. W.; King, R. W.; Burgen, A. S. V. Kinetics of Complex Formation Between Human Carbonic Anhydrase and Aromatic Sulfonamides. *Biochemistry* 1970, 9, 2638-2645.
- (25) Miller, J. M. *Chromatography: Concepts and Contrasts*; Wiley: New York, 1988; pp 25-39. Brainthwaite, A.; Smith, F. J. *Chromatographic Methods*; Chapman and Hall: New York, 1985; pp 11-23. Giddings, J. C. In *Chromatography*; Heftmann, E., Ed.; Van Nostrand Reinhold: New York, 1975; pp 27-45.
- (26) For a related simulation of time dependent distribution of solutes during development of a chromatographic run see: Stevens, F. J. Analysis of Protein-Protein Interaction by Simulation of Small-Zone Size-Exclusion Chromatography. Stochastic Formulation of Kinetic Rate Contributions to Observed High Performance Liquid Chromatography Elution Characteristics. *Biophys. J.* 1989, 55, 1155. Stevens, F. J. Analysis of Protein-Protein Interaction by Simulation of Small-Zone Size-Exclusion Chromatography. Application to Antibody-Antigen Association. *Biochemistry* 1986, 25, 981-993.
- (27) For related models for the transport behavior of protein interacting with mobile ligands on size exclusion HPLC see: Endo, S.; Hayashi, H.; Wada, A. Affinity Chromatography Without Immobilized Ligands; A New Method for Studying Macromolecular Interactions Using High-Performance Liquid Chromatography. *Anal. Biochem.* 1982, 124, 372-379. Endo, S.; Wada, A. Theoretical and Experimental Studies on Zone-Interference Chromatography as a New Method for Determining Macromolecular Kinetic Constants. *Biophys. Chem.* 1983, 18, 291-301.
- (28) For a more rigorous model for capillary zone electrophoresis of analytes that have invariant properties during the chromatographic run see: Dose, E. V.; Guiochon, G. A. High Resolution Modeling of Capillary Zone Electrophoresis and Isotachopheresis. *Anal. Chem.* 1991, 63, 1063-1072.
- (29) The electrophoretic mobility of the complex was estimated by extrapolating the electrophoretic mobility of CA at $[L] \rightarrow \infty$ using a curve-fitting program.
- (30) Time increments, Δt , in the simulation were chosen so that the concentration in any compartment does not change by more than 10% per equilibration step (eq 12); a significantly small value for Δt required a considerable amount of computer time, and a high value for Δt caused negative concentrations for CA in some compartments.
- (31) Slight deviation (<5%) of the value of the binding constant obtained by Scatchard analysis of the simulation-generated electropherograms from the value of the binding constant used in the simulation was observed when data representing low concentrations of ligand in the electrophoresis buffer (compared to the initial concentration of the enzyme) were included in the regression analysis. This deviation was more pronounced at lower concentrations of the ligand. Closer examination of the simulation indicated that this artifact was due to some amount of the total simulation time being used achieving equilibrium conditions. We also observe this trend experimentally: that is, data obtained at higher concentrations of ligand gave better fits on Scatchard analysis.
- (32) We have determined the rate of broadening of the peak (σ^2) as a function of time and have concluded that the broadening due to the additional 24 s of migration time should be negligible (<0.1%).
- (33) Previous determinations relied on fluorescence measurements or titration of products.
- (34) Several approaches have been reported to reduce protein adsorption in capillary electrophoresis: Towns, J. K.; Regnier, F. E. Polyethyleneimine-Bonded Phases in the Separation of Proteins by Capillary Electrophoresis. *J. Chromatogr.* 1990, 516, 69-78. Bruin, G. J. M.; Huisden, R.; Kraak, J. C.; Poppe, H. Performance of Carbohydrate-Modified Fused-Silica Capillaries for the Separation of Proteins by Zone Electrophoresis. *J. Chromatogr.* 1989, 480, 339-349. Towns, J. K.; Regnier, F. E. Capillary Electrophoretic Separations of Proteins Using Nonionic Surfactant Coatings. *Anal. Chem.* 1991, 63, 1126-1132. Mazzeo, J. R.; Krull, I. S. Capillary Isoelectric Focusing of Proteins in Uncoated Fused-Silica Capillaries Using Polymeric Additives. *Anal. Chem.* 1991, 63, 2852-2857. Bushey, M. M.; Jorgenson, J. W. Capillary Electrophoresis of Proteins in Buffers Containing High Concentrations of Zwitterionic Salts. *J. Chromatogr.* 1989, 480, 301-310. Zhu, M.; Rodriguez, R.; Hansen, D.; Wehr, T. Capillary Electrophoresis of Proteins Under Alkaline Conditions. *J. Chromatogr.* 1990, 516, 123-131.
- (35) The migration times can be corrected using migration indices see: Lee, T. T.; Yeung, E. S. Facilitating Data Transfer and Improving Precision in Capillary Zone Electrophoresis With Migration Indices. *Anal. Chem.* 1991, 63, 2842-2848. The effects of background noise can be minimized.¹³
- (36) Farrar, W. D. Reactions of Some Arenesulfonyl Chlorides. *J. Chem. Soc.* 1960, 3063-3069. El-Hewehi, Z.; Runge, F. Sulfonic Acid Derivatives: Preparation and Applicability as Mothproofing Agents. *J. Prakt. Chem.* 1962, 297-336.
- (37) Seto, C.; Mathias, J. P.; Whitesides, G. M. Molecular Self-Assembly Through Hydrogen Bond: Aggregation of Five Molecules To Form A Discrete Supramolecular Structure. *J. Am. Chem. Soc.* 1992, in press.